Redox Biology 5 (2015) 24–32

Contents lists available at ScienceDirect

Redox Biology

journal homepage: www.elsevier.com/locate/redox

Research Paper

Persistent oxidative stress in human neural stem cells exposed to low fluences of charged particles

Janet E. Baulch [1], Brianna M. Craver [1], Katherine K. Tran, Liping Yu, Nicole Chmielewski, Barrett D. Allen, Charles L. Limoli *

Department of Radiation Oncology, University of California, Irvine, CA 92697-2695, USA

ARTICLE INFO

Article history:
Received 4 March 2015
Accepted 10 March 2015
Available online 11 March 2015

Keywords:
Human neural stem cells
Oxidative stress
Charged particle
Space radiation

ABSTRACT

Exposure to the space radiation environment poses risks for a range of deleterious health effects due to the unique types of radiation encountered. Galactic cosmic rays are comprised of a spectrum of highly energetic nuclei that deposit densely ionizing tracks of damage along the particle trajectory. These tracks are distinct from those generated by the more sparsely ionizing terrestrial radiations, and define the geometric distribution of the complex cellular damage that results when charged particles traverse the tissues of the body. The exquisite radiosensitivity of multipotent neural stem and progenitor cells found within the neurogenic regions of the brain predispose the central nervous system to elevated risks for radiation induced sequelae. Here we show that human neural stem cells (hNSC) exposed to different charged particles at space relevant fluences exhibit significant and persistent oxidative stress. Radiation induced oxidative stress was found to be most dependent on total dose rather than on the linear energy transfer of the incident particle. The use of redox sensitive fluorogenic dyes possessing relative specificity for hydroxyl radicals, peroxynitrite, nitric oxide (NO) and mitochondrial superoxide confirmed that most irradiation paradigms elevated reactive oxygen and nitrogen species (ROS and RNS, respectively) in hNSC over a 1 week interval following exposure. Nitric oxide synthase (NOS) was not the major source of elevated nitric oxides, as the use of NOS inhibitors had little effect on NO dependent fluorescence. Our data provide extensive evidence for the capability of low doses of charged particles to elicit marked changes in the metabolic profile of irradiated hNSC. Radiation induced changes in redox state may render the brain more susceptible to the development of neurocognitive deficits that could affect an astronaut's ability to perform complex tasks during extended missions in deep space.

Introduction

Ionizing radiations come in many types and a critical property that distinguishes sparsely from densely ionizing radiations is stopping power, or the rate at which energy is deposited per unit track length. Linear energy transfer (LET), expressed in keV/μm, is the term used to classify radiation quality in terms of high versus low LET. With the exception of protons, the charged particles found in space fall into the high LET category [1,2]. These fully ionized, highly energetic nuclei are referred to as HZE particles, derived from high (H) atomic number (Z) and energy (E). While radiobiologist have quantified the differences among radiations of varying LET for numerous biological endpoints, characterizing similar responses for central nervous system (CNS) endpoints has proven more challenging [3]. LET dependent trends for changes in cognition, electrophysiology, neurogenesis and related biochemical and structural parameters have been difficult to demonstrate conclusively owing to the complexity of the CNS radiation response [3]. A large fraction of the brain is comprised of radioresistant, post-mitotic cells and at space relevant fluences, radiation induced changes transpire in the relative absence of cell death [4]. As a result, it is necessary to measure neuronal function and to identify biochemical changes that impact cognitive performance.

Despite the general radioresistance of the brain, the neurogenic regions contain crucial radiosensitive populations of neural stem and progenitor cells that can be depleted by exposures to relatively low doses of radiation [5,6]. While the radiation induced depletion of stem cell pools in the brain has been shown to disrupt neurogenesis and cognition at higher, clinically relevant doses of radiation [7,8], it is unclear whether similar effects will be observed following exposure to space radiations at doses expected to be incurred during short term or extended space travel. As NASA contemplates longer term missions beyond the protective

* Correspondence to: Department of Radiation Oncology, University of California Irvine, Medical Sciences I, Room B-146B, Irvine, CA 92697-2695, USA.
E-mail address: climoli@uci.edu (C.L. Limoli).
[1] These authors contributed equally to this work

http://dx.doi.org/10.1016/j.redox.2015.03.001

magnetosphere of Earth, the capability of charged particles to elicit changes in redox metabolism become increasingly important since biochemical changes capable of causing oxidative stress provide a mechanism for altering regional or global neurotransmission [9]. Considerable work from our laboratory has clearly demonstrated that radiations of varied quality (i.e. LET) elicit oxidative stress to differing extents [9–12]. Higher LET radiations were found to elicit more persistent and significant increases in oxidative stress than lower LET radiation modalities [9,12]. While these and other studies have characterized the capability of HZE particle exposure to elicit oxidative stress, they did not undertake a systematic study to determine how changes in LET and energy of different incident particles impact the onset and duration of radiation induced oxidative stress. Here we report our findings using human neural stem cells exposed to four different charged particles and three different energies to elucidate the microdosimetric relationships for the induction and persistence of oxidative stress.

Materials and methods

Cell culture

Low passage EnStem-A human neural stem cells (EMD Millipore, Billerica, MA) were cultured in flasks treated with poly-L-ornithine (20 μg/ml, Sigma-Aldrich, St. Louis, MO) and laminin (5 μg/ml, Sigma-Aldrich). Cells were maintained at 37 °C and 5% CO_2 in EnStem-A neural expansion media (EMD Millipore) containing neurobasal media supplemented with L-glutamine (2 mM, Invitrogen, Life Technologies, Grand Island, NY), basic fibroblast growth factor (20 ng/ml, EMD Millipore) and 1 × MEM non-essential amino acids (Life Technologies). These cells were routinely passaged 1:2 every other day.

Irradiation

One day prior to irradiation, cells were passaged into pre-coated T-25 flasks. These exponentially growing hNSC were either sham irradiated or exposed to 5–100 cGy doses of ^{16}O, ^{28}S, ^{48}Ti or ^{56}Fe particles (600 MeV/n; 10–50 cGy/min). For ^{28}Si and ^{56}Fe particles, energy escalations were also evaluated using 300, 600, 1000 MeV/n beams. Cells were irradiated at the NASA Space Radiation Laboratory (NSRL) at the Brookhaven National Laboratory, Upton, NY. All necessary dosimetry was provided by the Physics Dosimetry Group at the NSRL as previously described [9].

Cell survival analysis

Cell survival was determined using SYBR green fluorescence to quantify DNA using previously described protocols [9]. Briefly, following irradiation the hNSC were seeded into 24 well plates at a density of 50,000 cells per well, maintained for 5 days post-irradiation, and then frozen without media at −80 °C. Cells were then lysed using Mammalian Protein Extraction Reagent (Thermo Fischer Scientific, Waltham, MA) containing 2.5 × SYBR Green I (Invitrogen). SYBR Green I fluorescence was detected using a Synergy MX microplate reader and settings of 497 nm excitation and 520 nm emission (BioTek, Winooski, VT). Cell counts were determined by comparison to standard curves generated for the EnStem hNSC line. The data are presented as mean ± SD of at least 3 replicates after each had been normalized to its respective unirradiated control.

ATP assay

Following irradiation, hNSC were counted and seeded at 500,000 or 200,000 cells per well into coated 24 well plates for analysis at 3 or 7 days post-irradiation, respectively. The ATP assays were preformed as recommended in the manufacturer protocol (Perkin Elmer, Waltham, MA). Briefly, at the appropriate time point cells were lysed in their respective well using the ATPlite lysis buffer, shaken for 5 min and then frozen at −80 °C. Subsequently, luciferase assays were performed as described in the manufacture's protocol. The data are presented as mean ± SD of at least 3 replicates after each had been normalized to its respective unirradiated control.

Oxidative stress

The detection of intracellular ROS and RNS was based on the ability of live cells to oxidize fluorogenic dyes to their corresponding analog. Exponentially growing cells were treated with the ROS/RNS sensitive dye 5-(and-6)-chloromethyl-2′,7′-dichlorofluorescein diacetate (CM-H_2DCFDA or CM; 5 μM; Invitrogen), the nitric oxide sensitive dye 4-amino-5-methylamino-2′,7′-dichlorofluorescein diacetate (DAF; 5 μM; Invitrogen), or the superoxide sensitive dye Mito-SOX (MS; 0.5 μM; Invitrogen). Immediately after incubation with dye, cells were harvested and analyzed by flow cytometry. For each post-irradiation time, measurements of ROS/RNS (CM), NO (DAF), or superoxide (MS) in irradiated and sham irradiated control cultures were performed in parallel. All measurements were performed in triplicate from separate, independently irradiated flasks of cultured hNSC and the data presented as mean ± SD after each sample had been normalized to its respective unirradiated control.

Inhibition of nitric oxide synthases (NOS)

In order to determine whether nitric oxide synthases (NOS) contributed to radiation induced oxidative stress, hNSC were treated with either 100 μM of the NOS inhibitors L-N^5-(1-iminoethyl)ornithine hydrochloride (L-NIO, Sigma-Aldrich) or N^G-methyl-L-arginine acetate salt (L-NMMA, Sigma-Aldrich). Immediately following irradiation, NOS inhibitor drugs were prepared in culture medium and added to the cells. The cells subsequently received a media change containing freshly prepared inhibitor every 2–3 days and were maintained at 50% confluence until FACS analysis was performed. FACS analysis was performed on post-irradiation day 3 and on day 7 to measure oxidative stress.

Statistical analysis

For all assays, data for irradiated cells were normalized to that assay's sham irradiated concurrent control level for each time point. Data are presented as the mean of at least 3 replicate experiments ± SD. The data were assessed for significance (*i.e.* $P \leq 0.05$) by analysis of variance (ANOVA) with comparisons between groups performed using Bonferroni's post-hoc test using Prism3 software.

Results

Dose dependent survival in human neural stem cells

Human neural stem cells were irradiated with 600 MeV/n ^{28}Si or ^{56}Fe particles using a range of doses (0–100 cGy) to investigate the effects on cell proliferation. As compared to unirradiated controls, cell counts were not decreased by the 5 cGy dose of ^{28}Si particles, but were reduced significantly following the 25 and

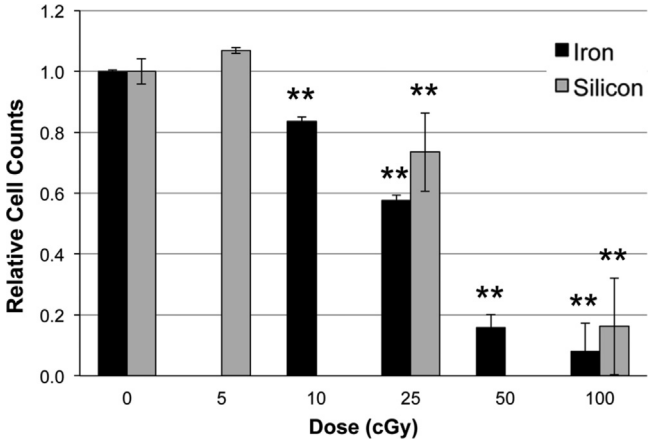

Fig. 1. Survival of hNSC following charged particle exposure. HNSC were exposed to various doses of ^{28}Si or ^{56}Fe particles exhibit dose dependent impairment of survival. $^{**}P < 0.001$ versus sham-irradiated control. All results are means of at least three independent experiments ± SD.

100 cGy doses (Fig. 1; −26%, and −84%, respectively). Using higher LET ^{56}Fe particles, we found that cell counts were significantly lower, 16%, 42%, 84%, and 92% for 10, 25, 50 and 100 cGy, respectively. While dose dependence for cell survival was observed, there was no evidence of LET dependence.

The effect dose and LET on ATP levels in irradiated human neural stem cells

Human neural stem cells were irradiated using 600 MeV/n ^{16}O, ^{28}Si and ^{56}Fe particles of increasing LET, then evaluated for changes in ATP (Fig. 2A). At 3 days post-irradiation, 5 and 25 cGy of ^{16}O particles increased ATP levels by 34% and 59%, respectively, while the 100 cGy dose reduced ATP levels −27% relative to controls (Fig. 2A). At this same time however, the higher LET ^{28}Si and ^{56}Fe particles induced dose dependent increases in ATP at all doses (^{28}Si: 28%, 44%, and 60% Fig. 2B; ^{56}Fe: 52%, 53%, and 71%; Fig. 2C). As with cell proliferation, no LET dependence was observed for changes in ATP levels.

In contrast to the trends observed 3 days post-irradiation, the ATP levels in cells exposed to 5 and 25 cGy doses of ^{16}O particles returned to control levels at day 7 post-irradiation, while cells irradiated with 100 cGy showed a decrease in ATP (−32% of control; Fig. 2A). Increased levels of ATP found 3 days after irradiation persisted at day 7 at the lower doses of ^{28}Si (24–32%), but were reduced by the 100 cGy dose (−6%; Fig. 2B). Cells exposed to ^{56}Fe particles exhibited reduced ATP levels at the lower doses (−23%) and higher dose (−89%) 7 days after exposure relative to unirradiated controls (Fig. 2C).

The effect of LET and radiation dose on oxidative stress in irradiated human neural stem cells

Cells were irradiated using 600 MeV/n ^{16}O, ^{28}Si, ^{48}Ti and ^{56}Fe charged particles to explore the effects of increasing LET on oxidative stress. At 3 days post-irradiation similar trends were generally observed for each particle, with oxidative stress increasing with dose (Fig. 3). Cells exposed to ^{56}Fe particles at 5 cGy exhibited significantly decreased CM fluorescence, indicative of ROS/RNS levels, compared to unirradiated controls (−14%; Fig. 3A), an effect also found with the other particles at that dose. While all particles induced significant increases in CM fluorescence at the 100 cGy dose, the ^{56}Fe particles induced the largest increase (100%, Fig. 3A). As indicated by DAF fluorescence, nitric oxide levels were significantly decreased (−17%) by the ^{48}Ti particles at 5 cGy

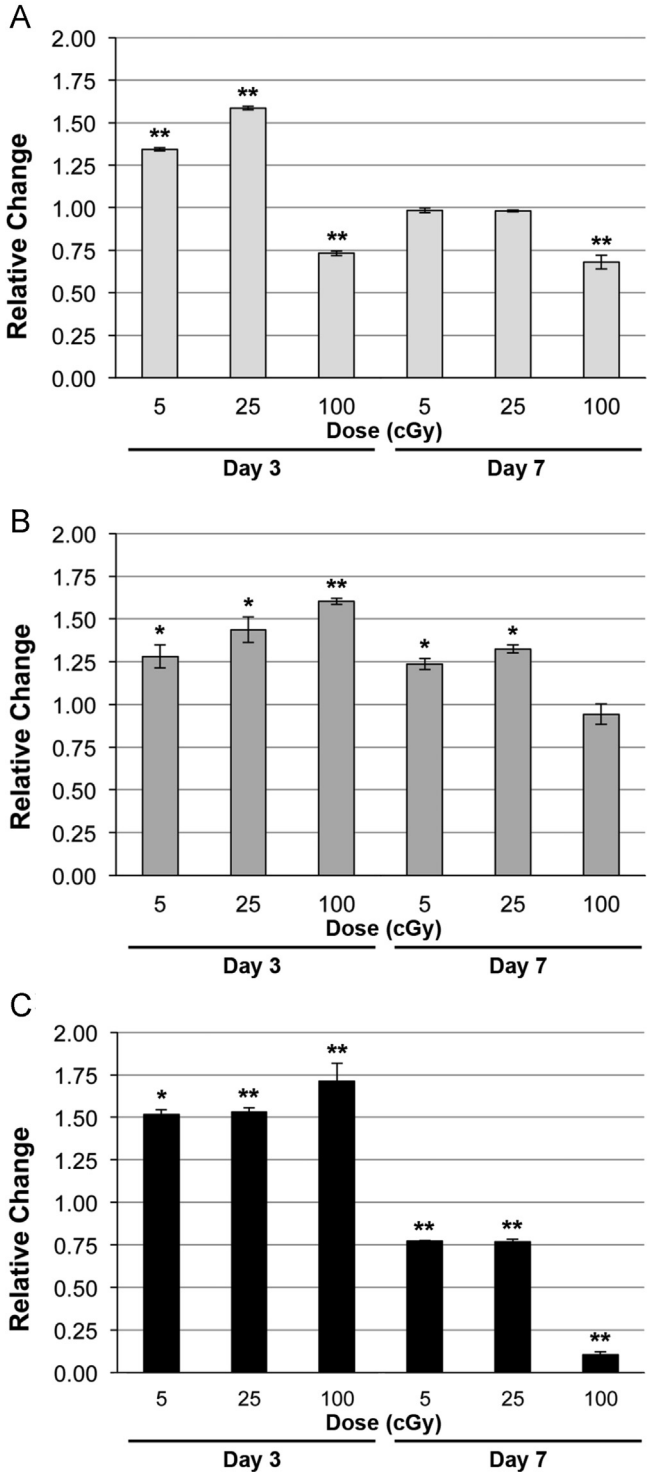

Fig. 2. ATP levels in hNSC following exposure to heavy charged particles of increasing LET. (A) ^{16}O, (B) ^{28}Si, (C) ^{56}Fe. Irradiated hNSC were evaluated for ATP levels 3 or 7 days post-exposure. All results are means of at least three independent experiments ± SD following normalization to each experiment's respective unirradiated control. $^{*}P < 0.05$, $^{**}P < 0.001$ by one way ANOVA followed by Bonferroni's multiple comparison test.

compared to the other ions and controls (Fig. 3B). Similarly, the 100 cGy dose increased nitric oxide levels for all particles by 87%, 64%, 47%, and 101% for ^{16}O, ^{28}Si, ^{48}Ti and ^{56}Fe particles respectively relative to controls (Fig. 3B). Interestingly, superoxide levels as measured by MS fluorescence were increased significantly with escalating LET at the 25 and 100 cGy doses 3 days post-irradiation

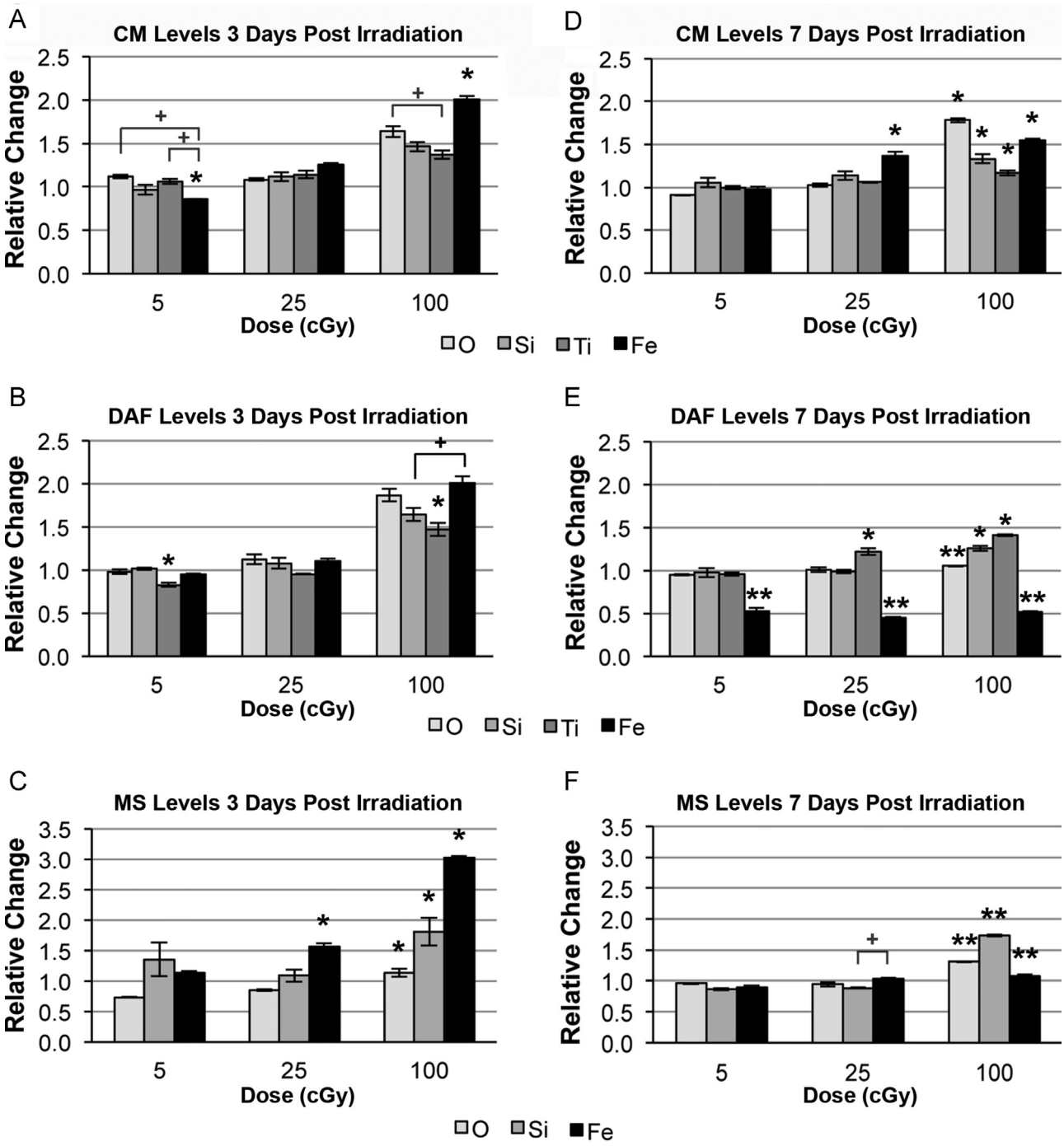

Fig. 3. Effect of dose and LET on oxidative stress in hNSC exposed to various charged particles (600 MeV/n) at 3 and 7 days post-irradiation. (A, D) Effect of LET on RNS/ROS using the CM dye at 3 and 7 days post-irradiation, respectively. (B, E) Effect of LET on NO using the DAF dye at 3 and 7 days post-irradiation, respectively. (C, F) Effect of LET on superoxide using the MS dye at 3 and 7 days post-irradiation, respectively. All results are means of at least three independent experiments ± SD following normalization to each experiment's respective unirradiated control. $^{*}P < 0.05$, $^{**}P < 0.001$ for comparison among particles for a given dose, and $^{+}P < 0.05$ between the noted particles, by one way ANOVA followed by Bonferroni's multiple comparison test.

(Fig. 3C). Exposure to 25 cGy of ^{56}Fe particles induced an increase of 56%, while the 100 cGy dose increased nitric oxide levels by 14%, 81% and 203% for ^{16}O, ^{28}Si, and ^{56}Fe particles, respectively, relative to control levels.

At 7 days post-irradiation, ROS/RNS generally increased with increasing dose (Fig. 3D). A 25 cGy dose of ^{56}Fe particles increased significantly ROS/RNS levels relative to the other particles at the same dose (37% of control). Increased levels of reactive species found 3 days after exposure to 100 cGy were again found to persist 7 days after irradiation, where ROS/RNS increased by 78%, 33%, 17% and 54% for ^{16}O, ^{28}Si, ^{48}Ti and ^{56}Fe particles, respectively, relative to controls (Fig. 3D). While all doses of ^{56}Fe particles induced significantly lower nitric oxide levels compared to other particles after 7 days (47%, 55% and 49%, respectively; Fig. 3E), other particles induced increased levels of nitric oxide at 25 cGy (22%, ^{48}Ti) and 100 cGy (25% and 40% for ^{28}Si and ^{48}Ti respectively; Fig. 3E). At 7 days after exposure there was a significant difference in superoxide levels among all three particles evaluated at the 100

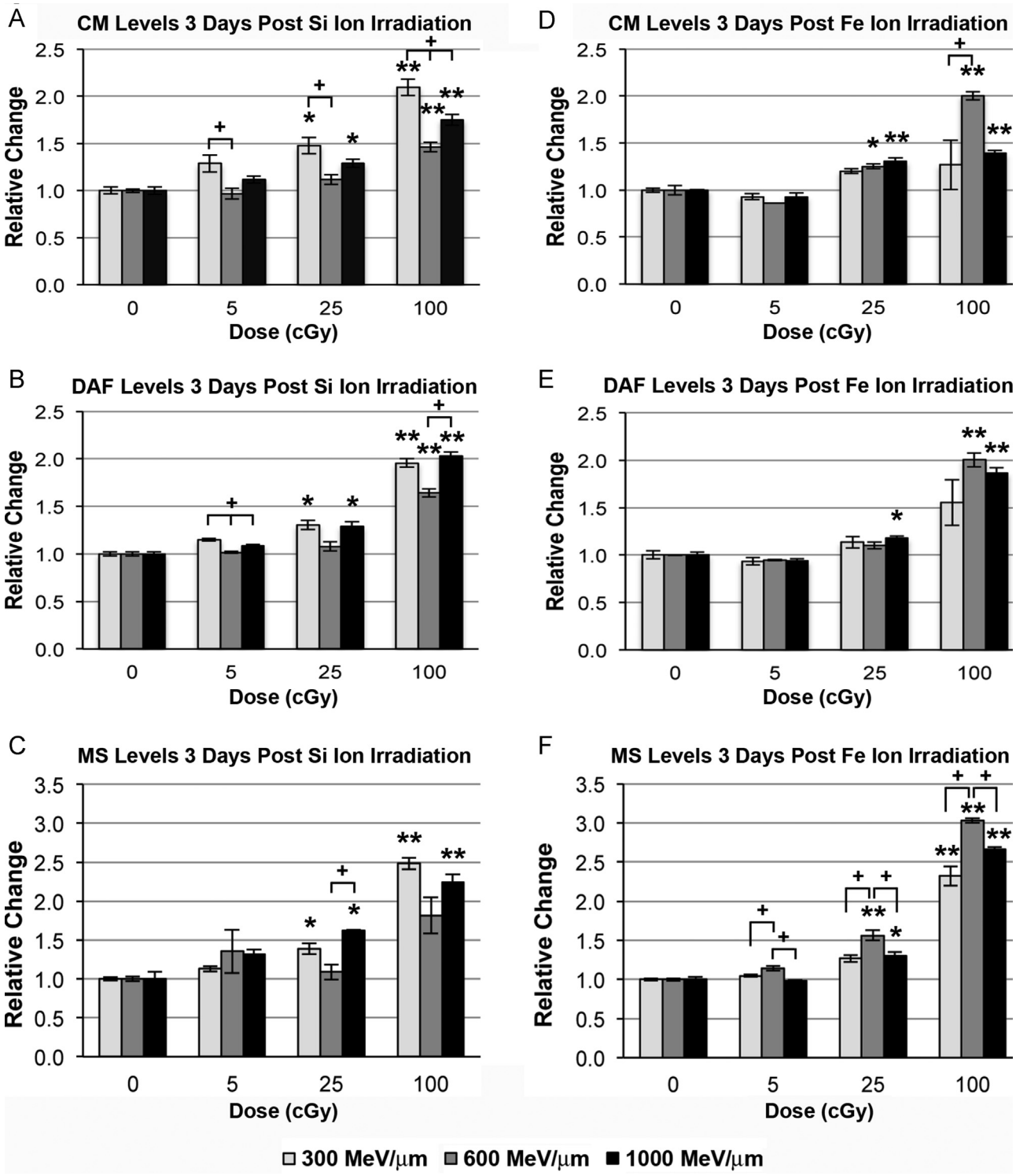

Fig. 4. Effect of energy escalation on oxidative stress in hNSC exposed to ^{28}Si and ^{56}Fe particles at 3 days post-irradiation. HNSC exposed to 5, 25 or 100 cGy of 300, 600 or 1000 MeV/n ^{28}Si or ^{56}Fe particles were evaluated for changes in levels of ROS/RNS, nitric oxide, and superoxide. (A, D) RNS/ROS using the CM dye. (B, E) NO using the DAF. (C, F) Superoxide using the MS dye. All results are means of at least three independent experiments ± SD following normalization to each experiment's respective unirradiated control. $^{*}P < 0.05$, $^{**}P < 0.001$ for comparison to control, and $^{+}P < 0.05$ between the noted particles for a given dose, by one way ANOVA followed by Bonferroni's multiple comparison test.

cGy dose relative to each other and to controls. However, increased superoxide at this time was only found after 100 cGy doses of ^{16}O and ^{28}Si particles (31% and 73%, respectively; Fig. 3F). Altogether these data suggest that dose rather than LET is the predominate factor dictating the level of charged particle induced oxidative stress in hNSC.

Effect of energy escalation on oxidative stress in hNSC

In order to determine the effects of energy escalation on oxidative stress, hNSC were irradiated with 5, 25, or 100 cGy of ^{28}Si or ^{56}Fe particles at 300, 600 or 1000 MeV/n, and then assessed for reactive species using our suite of redox sensitive dyes 3 or 7 days

later. At 3 days post-irradiation, hNSCs exposed to 25 or 100 cGy doses of 300 or 1000 MeV/n ^{28}Si particles had increased oxidative stress compared to cells with no irradiation (Fig. 4A–C). Exposure to 25 cGy of ^{28}Si particles increased ROS/RNS levels by 48% and 29% at 300 and 1000 MeV/n, respectively. These levels increased further at 100 cGy compared to controls (110%, 46%, and 75% at 300, 600, and 1000 MeV/n respectively; Fig. 4A). Nitric oxide levels were elevated significantly by 30% after exposure to 25 cGy of ^{28}Si particles at 300 or 1000 MeV/n, an effect that was increased further at 100 cGy (96%, 64% and 103% at 300, 600 and 1000 MeV/n respectively; Fig. 4B). Furthermore, superoxide levels increased significantly compared to controls after exposure to 25 cGy of 300

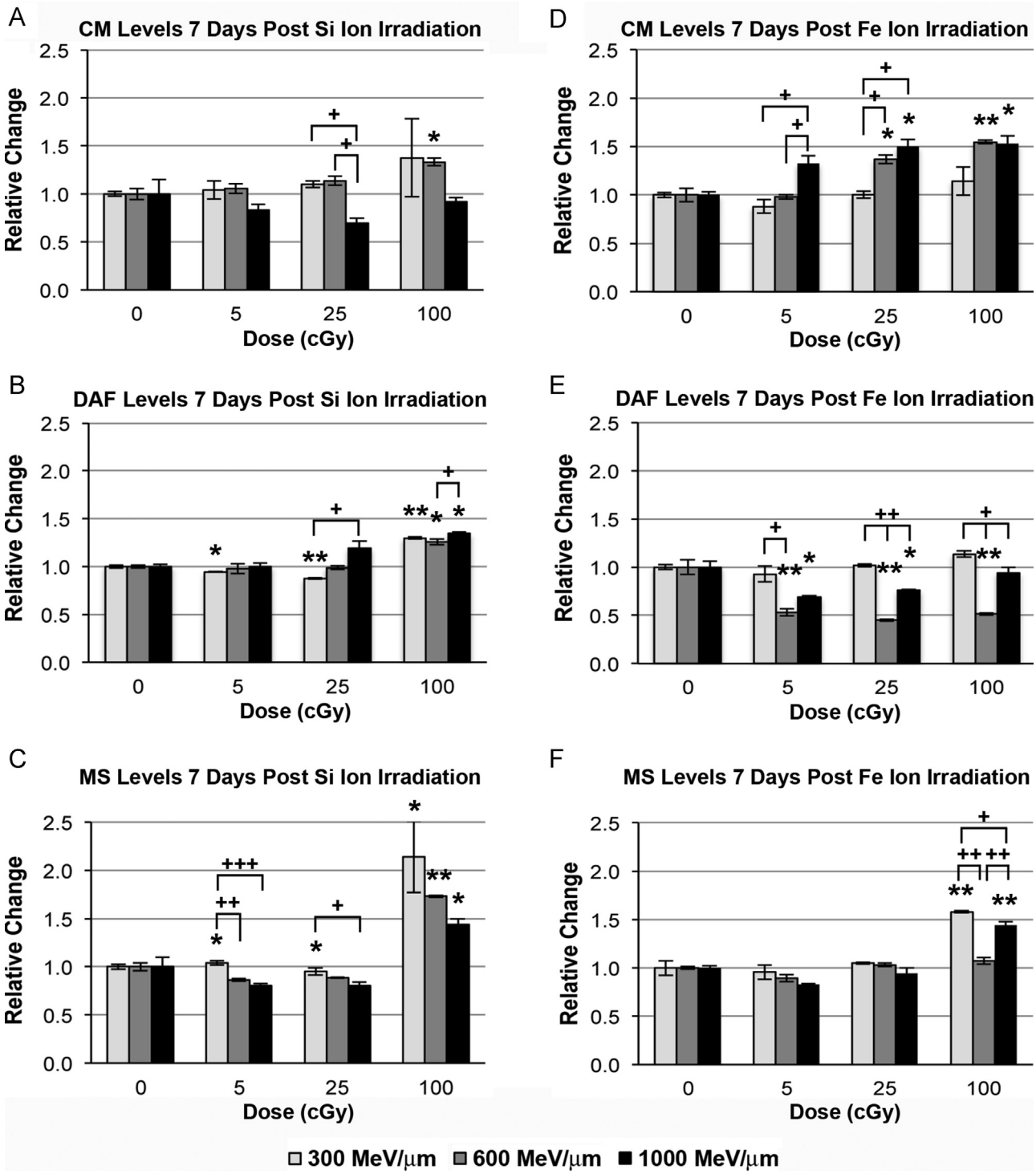

Fig. 5. Effect of energy escalation on oxidative stress in hNSC exposed to ^{28}Si and ^{56}Fe particles at 7 days post-irradiation. HNSC exposed to 5, 25 or 100 cGy of 300, 600 or 1000 MeV/n ^{28}Si or ^{56}Fe particles were evaluated for changes in levels of ROS/RNS, nitric oxide, and superoxide. (A, D) RNS/ROS using the CM dye. (B, E) NO using the DAF. (C, F) Superoxide using the MS dye. All results are means of at least three independent experiments ± SD following normalization to each experiment's respective unirradiated control. $^{*}P<0.05$, $^{**}P<0.001$ for comparison to control, and $^{+}P<0.05$, $^{++}P<0.001$ between the noted particles for a given dose, by one way ANOVA followed by Bonferroni's multiple comparison test.

and 1000 MeV/n ^{28}Si particles (39% and 62% respectively) and after exposure to 100 cGy (148%, 81%, and 124% at 300, 600, and 1000 MeV/n ^{28}Si particles respectively, Fig. 4C).

Three days after exposure to 25 cGy of ^{56}Fe particles, ROS/RNS levels increased by 25% and 31% at 600 and 1000 MeV/n respectively (Fig. 4D). Cells exposed to 100 cGy of ^{56}Fe particles using energies of 600 or 1000 MeV/n also showed significantly higher levels of ROS/RNS (100% and 39%, respectively). Nitric oxide levels were relatively unaffected 3 days after exposure to the lower doses of ^{56}Fe particles (with the exception of 25 cGy of ^{56}Fe particles at 1000 MeV/n) (Fig. 4E). However, cells irradiated with 100 cGy of ^{56}Fe particles exhibited significantly increased nitric oxide levels of 55%, 101% and 87% at 300, 600 or 1000 MeV/n, respectively (Fig. 4E). Relative to unirradiated controls, superoxide was also increased by 56% and 30% in cells exposed to 25 cGy of ^{56}Fe particles at 600 and 1000 MeV/n, as well as by 132%, 203% and 166% for each energy following exposure to 100 cGy of ^{56}Fe particles (Fig. 4F). Collectively these data again indicate that total dose was the predominate factor impacting radiation-induced oxidative stress, and while a dose response was generally observed, energy dependent trends were not found.

In general, the overall levels of reactive species were attenuated 7 days after exposure, but elevated ROS/RNS were still evident. At 7 days post-irradiation, ROS/RNS levels were increased by 33% using 100 cGy of 600 MeV/n ^{28}Si particles (Fig. 5A). Nitric oxide levels were decreased following exposure to 5 and 25 cGy of 300 MeV/n ^{28}Si particles (6% and 12%, respectively, Fig. 5B). However, 100 cGy doses of ^{28}Si particles increased NO levels by 30%, 26% and 35% at 300, 600 and 1000 MeV/n, respectively. Superoxide was decreased significantly following exposure to 5 and 25 cGy of 1000 MeV/n ^{28}Si particles (20%), but were increased relative to unirradiated controls at 100 cGy by 114%, 73% and 44% after exposure to 300, 600, and 1000 MeV/n ^{28}Si particles, respectively (Fig. 5C).

ROS/RNS levels were significantly elevated by 37% (5 cGy, 1000 MeV/n) and by 37% and 50% 7 days after exposure to 25 cGy of ^{56}Fe particles at 600 and 1000 MeV/n respectively. At these latter energies, exposure to 100 cGy of ^{56}Fe particles increased ROS/RNS levels by 54% and 53% (Fig. 5D). Using 600 MeV/n ^{56}Fe particles, doses of 5, 25, and 100 cGy decreased nitric oxide levels in irradiated hNSC by −47%, −55% and −49%, respectively (Fig. 5E). Furthermore, 1000 MeV/n ^{56}Fe particles also decreased nitric oxide levels by −31% and −24% 7 days after exposure to doses of 5 and 25 cGy. Increased superoxide levels were only observed after exposure to 100 cGy doses of ^{56}Fe particles at 300 and 1000 MeV/n (58% and 45%, respectively; Fig. 5F). Similar to the 3-day time point, no clear energy dependence was observed for

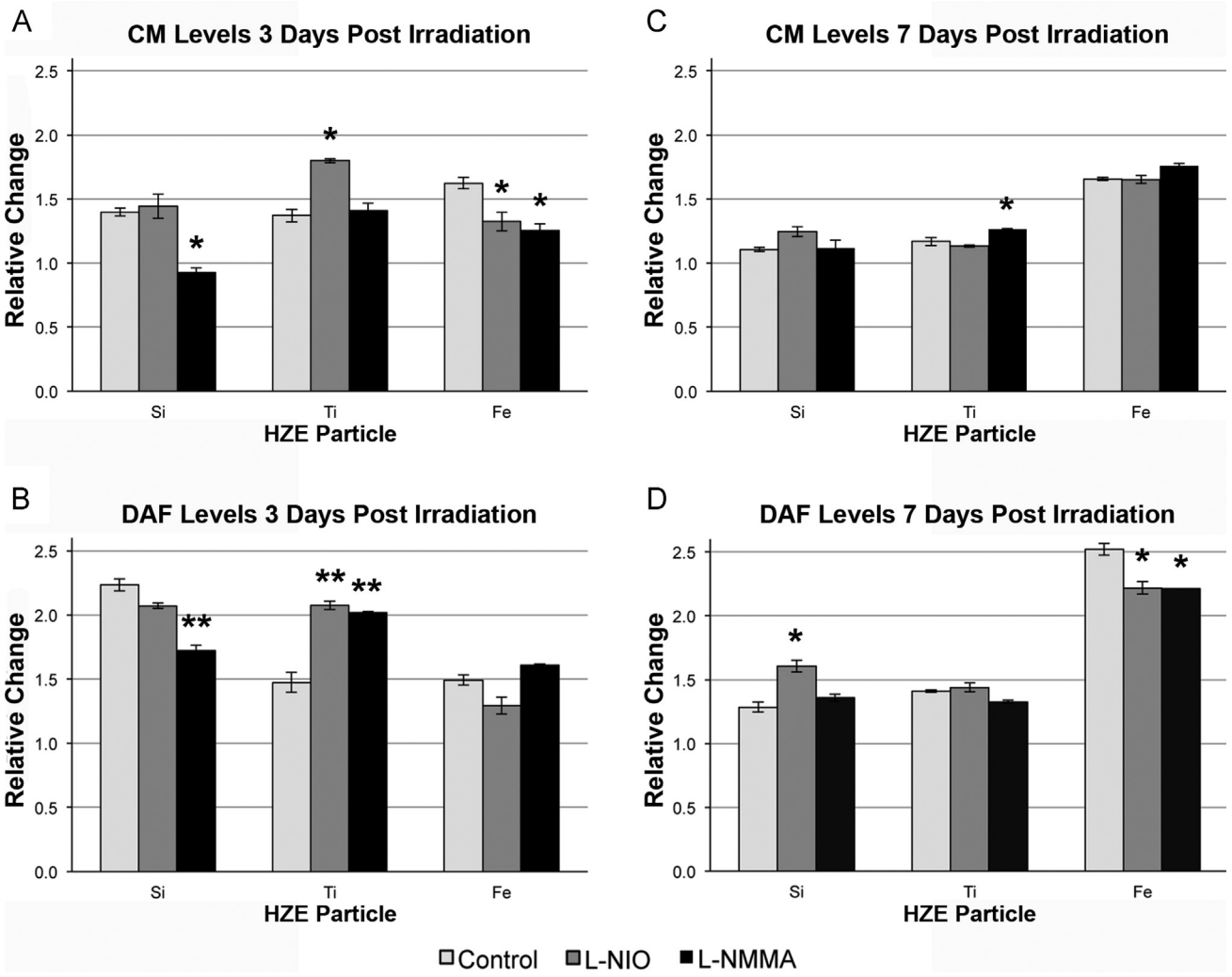

Fig. 6. Effect of NOS inhibitors (100 μM) on ROS/RNS and nitric oxide levels in hNSC exposed to various heavy particles (600 MeV/n, 100 cGy). Cells subjected to irradiation were incubated at 37 °C with 5 mM CM-H_2DCFDA or DAF-FM for 1 h, harvested and subjected to flow cytometric analysis. One way ANOVA followed by Bonferroni's multiple comparison test to compare 100 cGy irradiated samples with or without drug treatments relative to unirradiated controls, $^{*}P < 0.05$, $^{**}P < 0.001$.

charged particle induced oxidative stress 7 days following exposure.

Oxidative stress in irradiated cells treated with NOS inhibitors

To assess the potential contribution of NOS to the charged particle response, hNSCs were irradiated using ^{28}Si, ^{48}Ti or ^{56}Fe particles at a dose of 100 cGy and then treated with 100 μM L-NIO or L-NMMA every other day until oxidative stress levels were measured. Under nearly every condition (±drug), irradiation caused increased ROS/RNS and nitric oxide levels at 3 days post-irradiation that were differentially modulated by the NOS inhibitors (Fig. 6A, B). L-NMMA treatment decreased RNS/ROS levels after exposure to ^{28}Si (−36%) and ^{56}Fe (−26%) particles compared irradiated, but non-drug treated cells (Fig. 6A). L-NIO treatment gave mixed results, where ROS/RNS levels were found to increase (28%) or decrease (−24%) after ^{48}Ti or ^{56}Fe particle exposure, respectively (Fig. 6A). At 3 days post-irradiation, L-NMMA treatment caused a 23% decrease in NO relative to untreated hNSC irradiated with ^{28}Si particles (Fig. 6B). Both inhibitors increased relative levels of NO by 25% after exposure to ^{48}Ti particles (Fig. 6B). Exposure to ^{56}Fe particles in the presence of the drugs had relatively no effect at 3 days post-irradiation.

Similar to the earlier time point, radiation-induced oxidative stress was evident under most conditions 7 days after exposure, and was most pronounced after irradiation with 100 cGy of ^{56}Fe particles (Fig. 6C, D). Levels of ROS/RNS and NO were found to rise after ^{48}Ti and ^{28}Si exposure and treatment with L-NMMA or L-NIO respectively (Fig. 6C, D). The NOS inhibitors were only found to lower NO levels (−10%) after exposure of hNSC to ^{56}Fe particles (Fig. 6D). The remaining NOS inhibitor treatments for both time points showed no significant differences between treatment groups. Collectively, no discernable trends were evident between irradiated hNSCs treated with NOS inhibitors, suggesting that the impact of NOS to charged particle induced oxidative stress was insignificant under our experimental conditions.

Discussion

The present report provides conclusive evidence that exposure of hNSC to HZE particles elicits persistent oxidative stress. These data corroborate past studies using both high and low LET radiation types that show the ability of varied irradiation paradigms to elicit oxidative stress in cultured cells and in the intact brain [9–12]. Due to the high metabolic activity and utilization of oxygen, relatively modest disruptions to the redox homeostasis of the brain have the potential to precipitate deleterious and long-lasting perturbations to function [13]. Importantly, elevated levels of transient reactive species found over extended post-irradiation intervals occurred over fluence levels that only reduced survival within 1-log kill (Fig. 1). Despite the prevalence of reactive species, these are not likely to contribute significantly to cell kill following low dose exposures, as DNA DSB production remains the principal cause of radiation-induced kill under the experimental conditions [14]. Similarly, low dose exposures reported here did not lead to any significant reductions in ATP production, suggesting that the integrity of oxidative phosphorylation was not severely disrupted (Fig. 2). Thus, under conditions where the majority of cells survive and exhibit significant metabolic activity, increased levels of ROS and RNS were found to persist 3–7 days following acute exposure (Figs. 3–5).

To elucidate potentially important differences between multiple HZE particles delivered over a range of GCR relevant energies, current studies sought to determine whether radiation induced oxidative stress was dependent on LET. To date, few systematic investigations focused on CNS relevant cell types have utilized different HZE particles delivered at escalating energies [9,15–17]. Current findings suggest that total dose predominates as the factor most critical for subsequent development of elevated ROS and RNS detected through the use of redox sensitive fluorogenic dyes. Compared to sham irradiated controls, HZE particle exposure caused a number of significant changes to the redox metabolism of hNSCs. The highest levels of reactive species were routinely found after exposure to the larger doses (25, 100 cGy), regardless of whether cells were assayed 3 or 7 days following exposure (Figs. 3 and 4). Radiation induced oxidative stress showed little or no dependence on the incident energy of the particle (300–1000 MeV/n), and with the exception of mitochondrial-derived superoxide 7 days following ^{28}Si exposure (Fig. 4F), energy dependent trends for changes in ROS or RNS levels were not found to be statistically different (Figs. 3 and 4). Thus, as the range of delta rays emanating from the track core increase as a function of particle energy [2,18], LET decreases, and data show little evidence that radiation induced changes in oxidative stress are overly dependent on such energy dependent changes in microdosimetry.

Further support for the relative independence of radiation induced oxidative stress on particle LET comes from the direct comparison of ROS and RNS levels found 3 or 7 days after exposure to 600 MeV/n ^{16}O, ^{28}Si, ^{48}Ti or ^{56}Fe HZE particles. In almost every instance, the highest levels of reactive species were found after the highest total dose of 100 cGy, with relatively little dependence on particle LET (Fig. 5). The only exception was observed for the generation of mitochondrial superoxide 3 days after exposure, where increased LET associated with higher atomic mass gave rise to escalating levels of superoxide (Fig. 5C). Overall however, data shown using 4 different HZE particles at the same energy uncovered little evidence in support of the idea that radiation induced oxidative stress was strictly dependent on particle LET.

To ascertain the potential source of elevated ROS/RNS following irradiation, additional studies focused on the potential role of nitric oxide synthase (NOS) uncoupling. Normally one of the 3 isoforms of NOS (i.e. nNOS, eNOS, iNOS) catalyzes the conversion of L-arginine to L-citrulline to produce NO in the presence of the appropriate co-factors [19]. Under certain circumstances this reaction can be “uncoupled” where NOS removes an electron from L-arginine and donates it to molecular oxygen to yield superoxide instead of NO [20]. Studies using NOS inhibitors (L-NIO and L-NMMA) at concentrations in excess of substrate (i.e. L-arginine) did not elicit significant changes in ROS/RNS levels (Fig. 6). While the presence of these NOS inhibitors did not preclude the occurrence of radiation induced oxidative stress over a 1 week interval, there were no consistent trends among the various particles used when compared to untreated controls. Thus, data suggest that NOS uncoupling does not play a predominate role in the radiation induced metabolic perturbations leading to increased ROS/RNS in multipotent hNSCs.

The quantification of radiation-induced oxidative stress through the use of fluorogenic dyes provides a convenient and useful measure for assessing overall changes in the redox status of cells. For offsite experimentation designed to quantify the effects of multiple charged particle types, this methodology provides an ideal avenue for determining whether redox changes are dependent on intrinsic differences in charged particles. These methodologies are not however without caveats, and their use to discriminate between specific reactive species is limited due to the complexity of the intracellular redox chemistry involved [21–23]. While cells analyzed in this study were not cultured under physiologic oxygen tension, all data were derived under similar controlled culture conditions. Thus, while fluorescent signals derived from oxidized dyes may be due to multiple reactive species

derived from different intracellular sources, utilization of these dyes does provide useful information barring over-interpretation.

Elucidating microdosimetric signatures dependent on particle LET in the CNS have proven difficult [3]. The structural and synaptic plasticity of the CNS in response to irradiation further confound efforts to assign/link differences in track structure to the radioresponse of functional endpoints in the CNS [9,24,25]. Primary and secondary ionizations associated with HZE particle traversals elicit significant metabolic perturbation to hNSCs that cause persistent increases in reactive species. While elucidating the precise identity and yields of specific ROS and RNS species requires a different approach, there is little doubt based on current and past work that energy deposition events caused by charged particle irradiation elicit oxidative stress. The capability of oxidative stress to impact the functionality of nearly any tissue has been substantiated over many years, and the CNS is no exception [3,6,13]. The balance between pro- and antioxidants in the brain affects decisions of proliferation and differentiation [26], and influences secondary reactive processes such as inflammation that regulate the remodeling of irradiated tissue during the repair of injury. Past data has shown the functional importance of altered redox state on a variety of endpoints that impact neurocognitive reserve, and changes reported here lend support to the idea that radiation induced oxidative stress constitutes a biochemical mechanism capable of altering neurotransmission both locally and globally over extended times following exposure to the space radiation environment.

Acknowledgements

This work was supported by NASA Grants NNA06CB39G, NX09AK25G and NNX10AD59G (CLL) and NNX13AK69G and NNX13AK70G (JEB). We thank Erich Giedzinski for his excellent technical assistance.

References

[1] S.B. Curtis, J.R. Letaw, Galactic cosmic rays and cell-hit frequencies outside the magnetosphere, Advances in Space Research 9 (10) (1989) 293–298. http://dx.doi.org/10.1016/0273-1177(89)90452-3 11537306.

[2] I. Plante, F.A. Cucinotta, Energy deposition and relative frequency of hits of cylindrical nanovolume in medium irradiated by ions: Monte Carlo simulation of tracks structure, Radiation and Environmental Biophysics 49 (1) (2010) 5–13. http://dx.doi.org/10.1007/s00411-009-0255-7 19916014.

[3] F.A. Cucinotta, M. Alp, F.M. Sulzman, M. Wang, Space radiation risks to the central nervous system, Life Sciences in Space Research 2 (2014) 54–69. http://dx.doi.org/10.1016/j.lssr.2014.06.003.

[4] J.R. Fike, S. Rosi, C.L. Limoli, Neural precursor cells and central nervous system radiation sensitivity, Seminars in Radiation Oncology 19 (2) (2009) 122–132. http://dx.doi.org/10.1016/j.semradonc.2008.12.003 19249650.

[5] C.S. Wong, A.J. Van der Kogel, Mechanisms of radiation injury to the central nervous system: implications for neuroprotection, Molecular Interventions 4 (5) (2004) 273–284. http://dx.doi.org/10.1124/mi.4.5.7 15471910.

[6] P.J. Tofilon, J.R. Fike, The radioresponse of the central nervous system: a dynamic process, Radiation Research 153 (4) (2000) 357–370. http://dx.doi.org/10.1667/0033-7587(2000)153[0357:TROTCN]2.0.CO;2 10798963.

[7] S. Mizumatsu, M.L. Monje, D.R. Morhardt, R. Rola, T.D. Palmer, J.R. Fike, Extreme sensitivity of adult neurogenesis to low doses of X-irradiation, Cancer Research 63 (14) (2003) 4021–4027 12874001.

[8] R. Rola, J. Raber, A. Rizk, S. Otsuka, S.R. VandenBerg, D.R. Morhardt, J.R. Fike, Radiation-induced impairment of hippocampal neurogenesis is associated with cognitive deficits in young mice, Experimental Neurology 188 (2) (2004) 316–330. http://dx.doi.org/10.1016/j.expneurol.2004.05.005 15246832.

[9] B.P. Tseng, E. Giedzinski, A. Izadi, T. Suarez, M.L. Lan, K.K. Tran, M.M. Acharya, G.A. Nelson, J. Raber, V.K. Parihar, C.L. Limoli, Functional consequences of radiation-induced oxidative stress in cultured neural stem cells and the brain exposed to charged particle irradiation, Antioxidants & Redox Signaling 20 (9) (2014) 1410–1422. http://dx.doi.org/10.1089/ars.2012.5134 23802883.

[10] E. Giedzinski, R. Rola, J.R. Fike, C.L. Limoli, Efficient production of reactive oxygen species in neural precursor cells after exposure to 250 MeV protons, Radiation Research 164 (4 2) (2005) 540–544. http://dx.doi.org/10.1667/RR3369.1 16187784.

[11] C.L. Limoli, E. Giedzinski, R. Rola, S. Otsuka, T.D. Palmer, J.R. Fike, Radiation response of neural precursor cells: linking cellular sensitivity to cell cycle checkpoints, apoptosis and oxidative stress, Radiation Research 161 (1) (2004) 17–27. http://dx.doi.org/10.1667/RR3112 14680400.

[12] C.L. Limoli, E. Giedzinski, J. Baure, R. Rola, J.R. Fike, Redox changes induced in hippocampal precursor cells by heavy ion irradiation, Radiation and Environmental Biophysics 46 (2) (2007) 167–172. http://dx.doi.org/10.1007/s00411-006-0077-9 17103219.

[13] A. Lewén, P. Matz, P.H. Chan, Free radical pathways in CNS injury, Journal of Neurotrauma 17 (10) (2000) 871–890. http://dx.doi.org/10.1089/neu.2000.17.871 11063054.

[14] M.M. Acharya, M.L. Lan, V.H. Kan, N.H. Patel, E. Giedzinski, B.P. Tseng, C. L. Limoli, Consequences of ionizing radiation-induced damage in human neural stem cells, Free Radical Biology and Medicine 49 (12) (2010) 1846–1855. http://dx.doi.org/10.1016/j.freeradbiomed.2010.08.021 20826207.

[15] K. Nojima, M.E. Vazquez, S. Nagaoka, Effects of low dose particle radiation to mouse neonatal neurons in culture, Uchu Seibutsu Kagaku 17 (3) (2003) 263–264 14676408.

[16] K. Nojima, T. Nakadai, Y. Kohno, M.E. Vazquez, N. Yasuda, S. Nagaoka, Effects of heavy ion to the primary [correction of rimary] culture of mouse brain cells, Uchu Seibutsu Kagaku 18 (3) (2004) 114–115 15858347.

[17] P. Grabham, P. Sharma, A. Bigelow, C. Geard, Two distinct types of the inhibition of vasculogenesis by different species of charged particles, Vascular Cell 5 (1) (2013) 16. http://dx.doi.org/10.1186/2045-824X-5-16 24044765.

[18] I. Plante, A. Ponomarev, F.A. Cucinotta, 3D visualisation of the stochastic patterns of the radial dose in nano-volumes by a Monte Carlo simulation of HZE ion track structure, Radiation Protection Dosimetry 143 (2–4) (2011) 156–161. http://dx.doi.org/10.1093/rpd/ncq526 21199826.

[19] U. Forstermann, W.C. Sessa, Nitric oxide synthases: regulation and function, European Heart Journal 33 (7) (2012) 829–837. http://dx.doi.org/10.1093/eurheartj/ehr304.

[20] N.D. Roe, J. Ren, Nitric oxide synthase uncoupling: a therapeutic target in cardiovascular diseases, Vascular Pharmacology 57 (5–6) (2012) 168–172. http://dx.doi.org/10.1016/j.vph.2012.02.004 22361333.

[21] B. Kalyanaraman, V. Darley-Usmar, K.J. Davies, P.A. Dennery, H.J. Forman, M. B. Grisham, G.E. Mann, K. Moore, L.J. Roberts 2nd, H. Ischiropoulos, Measuring reactive oxygen and nitrogen species with fluorescent probes: challenges and limitations, Free Radical Biology and Medicine 52 (1) (2012) 1–6. http://dx.doi.org/10.1016/j.freeradbiomed.2011.09.030 22027063.

[22] P. Wardman, Use of the dichlorofluorescein assay to measure “reactive oxygen species”, Radiation Research 170 (3) (2008) 406–407. http://dx.doi.org/10.1667/RR1439a.1 18763870.

[23] P. Wardman, Methods to measure the reactivity of peroxynitrite-derived oxidants toward reduced fluoresceins and rhodamines, Methods in Enzymology 441 (2008) 261–282. http://dx.doi.org/10.1016/S0076-6879(08)01214-7 18554539.

[24] V.K. Parihar, J. Pasha, K.K. Tran, B.M. Craver, M.M. Acharya, C.L. Limoli, Persistent changes in neuronal structure and synaptic plasticity caused by proton irradiation, Brain Structure & Function 220 (2015) 1161–1171. http://dx.doi.org/10.1007/s00429-014-0709-9 24446074.

[25] V.K. Parihar, B.D. Allen, K.K. Tran, N.N. Chmielewski, B.M. Craver, V. Martirosian, J.M. Morganti, S. Rosi, R. Vlkolinsky, M.M. Acharya, G.A. Nelson, A.R. Allen, C.L. Limoli, Targeted overexpression of mitochondrial catalase prevents radiation-induced cognitive dysfunction, Antioxidants & Redox Signaling 22 (2015) 78–91. http://dx.doi.org/10.1089/ars.2014.5929 24949841.

[26] J. Smith, E. Ladi, M. Mayer-Proschel, M. Noble, Redox state is a central modulator of the balance between self-renewal and differentiation in a dividing glial precursor cell, Proceedings of National Academy of Sciences of the United States of America 97 (18) (2000) 10032–10037. http://dx.doi.org/10.1073/pnas.170209797 10944195.